

THE INTERNATIONAL JOURNAL OF SCIENCE & TECHNOLEDGE

Study of Power Flow Solutions and ATC of Fixed Speed Wind Turbine Generating Systems

Syed Alla Bakshu

P. G. Student [EPS], Department of EEE, QUBA Engineering Collage,
Venkatachalam, SPSR Nellore (D), Andhra Pradesh, India

Shaik Hameed

Assistant Professor, Department of EEE, QUBA Engineering Collage,
Venkatachalam, SPSR Nellore (D), Andhra Pradesh, India

Abstract:

Now a days power generation from the renewable energy sources is increasing rapidly so generating the wind power and incorporating that into the power systems into power grid calls for proper modeling of the systems and incorporating the model into various computational tools used in power system operation and planning studies. This paper proposes a simple method of incorporating the exact equivalent circuit of a fixed speed wind generator into conventional power flow program. The method simply adds two internal buses of the generator to include all parameters of the equivalent circuit. For a given wind speed, the active power injection into one of the internal buses is determined through wind turbine power curve supplied by the manufacturers. The internal buses of the model can be treated as a traditional P-Q bus and thus can easily be incorporated into any standard power flow program by simply augmenting the input data files and without modifying source codes of the program. Available Transfer Capacity (ATC) of the power system also observed without and with fixed speed wind generator. The effectiveness of the proposed method is well discussed with various cases on the IEEE 24 bus and 30-bus system. And we also modeling a simple system which is connected to a infinite bus

Keywords: fixed speed wind turbine, P-Q bus, ATC

1. Introduction

The power generation from the renewable energy sources is increasing rapidly in recent years especially in that Wind is the fastest growing renewable energy technology in the world and is considered as the most cost effective way of generating electrical power from renewable sources. The principle of a wind turbine generating system (WTGS) is based on two well known processes: conversion of kinetic energy of moving air into mechanical energy, and conversion of mechanical energy into electrical energy. The integration of WTGS into power grid has increased significantly in recent years [1]. In fact, worldwide installation of wind turbines has increased from about 5 GW in 1995 to more than 275 GW in 2012 [2]. Increased penetration of wind generators into power grid calls for proper modeling of the WTGS and incorporating the model into various computational tools used for steady state and dynamic analyses of power systems. A WTGS can be classified into fixed speed, limited variable speed and variable speed [3,4]. The fixed speed (or Type-1) generating system employs a squirrel-cage induction generator (SCIG) which is directly connected to the grid through a step-up transformer. A soft starter and shunt capacitors are usually used for smoother connection and reactive power support. A SCIG operates within a very narrow speed range (around the synchronous speed) and that is why it is considered as a fixed speed generator. The limited variable speed (or Type-2) generating system employs a wound-rotor induction generator (WRIG). The speed of the generator can be varied within a certain range by adjusting external rotor impedance of the generator. The variable speed generating system requires either partial-size or full-size converters. The generating system with partial-size converters (or Type-3) employs a doubly feed induction generator (DFIG). The rotor excitation of the DFIG is supplied by a current regulated voltage source converter, which adjusts the magnitude and phase angle of rotor current almost instantly. The rotor side converter is connected back-to-back to a grid side converter. The generating system with full-size converter (or Type-4) usually employs a permanent magnet synchronous generator (PMSG), which is connected to the grid through full size back-to-back voltage source converters or a diode rectifier and a voltage source converter. In terms of power control, a wind turbine (WT) can be classified into stall-controlled and pitch-controlled [5,6]. A stall-controlled WT has a fixed blade angle but the blades are carefully designed to reduce aerodynamic efficiency at higher wind speeds to prevent the extraction of excessive power from the wind. On the other hand, a pitch-controlled WT adjusts the blade pitch angle to limit the power capture at higher wind speeds. Most of the earlier wind farms used fixed speed stall-controlled wind turbines [7]. A fixed speed WT is also known as “Danish concept” as it was developed and widely used in Danish wind farms. However, the present trend is to use variable speed WTs that employ DFIGs. In both cases, it is very important to incorporate the model of WTGS into existing computational tools used in power system studies.

The steady state behavior of a power system is usually evaluated through power flow calculations which mainly determine the complex voltage (magnitude and phase angle) of all buses. The complex power flow through each branch and other quantities are

then calculated using the complex bus voltages. In power flow calculations, the buses of a power system are classified into swing (or V-d) bus, voltage-controlled (or P-V) bus and load (or P-Q) bus [8,9]. For a P-V or a P-Q bus, the active power injection P into the bus is known or specified. Fortunately, most of the WT manufacturers provide the power curve (mechanical power versus wind speed) of the turbine [10, 11]. By knowing wind speed, the corresponding turbine mechanical power can immediately be determined from the curve. In power flow analysis, a fixed speed wind generating system is usually represented by a P-Q model or an R-X model [12–16]. In P-Q model, the reactive power drawn by the generator is first approximated in terms of its active power and terminal voltage. The per-phase steady state equivalent circuit of the generator, with some approximations, is used for this purpose. For a given wind speed, the generator bus is treated as a P-Q bus with varying reactive power, in contrast to a conventional P-Q bus where it remains constant. This model may not provide correct results because of the approximations used in evaluating the reactive power. An accurate P-Q model of a SCIG is described in [16] but the model need to be evaluated as a part of the iterative process of the power flow program. A DFIG or a PMSG can also be represented by a P-Q model with varying reactive power as it is controlled by the converter. Such generators can also be operated either as constant power factor mode or constant voltage mode. In R-X model, a SCIG generator is represented by an equivalent impedance obtained from its steady state equivalent circuit [12,13]. In power flow analysis, the impedance is then considered as a shunt element at the generator terminal bus. However, the impedance of the generator is not constant but highly dependent on operating slip which is not known a priori. In [12], a sub-problem is formulated to calculate the slip iteratively. Alternatively, the jacobian of the power flow program can be modified to include the slip [17]. In both cases, significant modifications to the source codes of the program are needed. This paper proposes a simple method of incorporating the exact equivalent circuit of a fixed speed wind generator into a power flow program that does not require any modification to source codes of the program. The ATC of the system is also observed based on the algorithm in [29] without and with wind generator. The proposed method is then tested and discussed well on the IEEE 24 bus and 30-bus systems. By changing the wind speed and checking the corresponding active power and reactive power injections and the terminal voltage of the system.

2. Power flow method

Power flow is nothing but how the terms in the line are changing according to the conditions happened either in load side or in generation side how there changing according to the wind speed . Power flow is one of the most important computational tools used in power system operation and planning studies. It solves the active and reactive power equations to find bus voltage magnitudes and phase angles. The injected active power (P_i) and reactive power (Q_i) into bus i of an n -bus power system can be written as [8].

$$P_i = V_i^2 G_{ii} + V_i \sum_{j=1, j \neq i}^n V_j (B_{ij} \sin \delta_{ij} + G_{ij} \cos \delta_{ij}) \quad (1) \quad Q_i = -V_i^2 B_{ii} + V_i \sum_{j=1, j \neq i}^n V_j (G_{ij} \sin \delta_{ij} - B_{ij} \cos \delta_{ij}) \quad (2)$$

Here $Y = (G + jB)$ and $\delta_{ij} = (\delta_i - \delta_j)$. V_i and V_j are the voltage magnitude of buses i and j , respectively. δ_i and δ_j are the voltage phase angle of buses i and j , respectively, and Y is the bus admittance matrix. The Newton Raphson (NR) method is commonly used to solve the above equations. The governing equation of the method can be written as

$$\begin{bmatrix} \Delta P \\ \Delta Q \end{bmatrix} = \begin{bmatrix} \frac{\partial P}{\partial \delta} & \frac{\partial P}{\partial V} \\ \frac{\partial Q}{\partial \delta} & \frac{\partial Q}{\partial V} \end{bmatrix} \begin{bmatrix} \Delta \delta \\ \Delta V \end{bmatrix} \equiv [J] \begin{bmatrix} \Delta \delta \\ \Delta V \end{bmatrix} \quad (3)$$

The size of the jacobian matrix J in (3) is $(n_{PV} + 2n_{PQ}) \times (n_{PV} + 2n_{PQ})$, where n_{PV} is the number of P-V buses and n_{PQ} is the number of P-Q buses in the system. The computational algorithm of the method is well described in literature [8,9]. For most of the well-behaved systems, the NR method usually converges in 3–6 iterations.

3. Wind power

The wind turbine converts the wind energy in electrical by capturing the kinetic energy from the wind and converting it into mechanical energy. The mechanical power captured by a wind turbine (P_T) can be written as [18, 19].

$$P_T = \frac{1}{2} \rho A V_w^3 C_p(\lambda, \beta) \quad (4)$$

Here ρ is the air density (kg/m^3), A is the turbine blade swept area (m^2), V_w is the wind speed (m/s), and C_p is the performance coefficient of the turbine. C_p is a function of tip speed ratio k and bladepitch angle b , and it can be expressed as [19]

$$C_p(\lambda, \beta) = c_1 \left[\frac{c_2}{\lambda_i} - c_3 \beta - c_4 \beta^c - c_5 \right] e^{-\frac{c_7}{\lambda_i}} \quad (5)$$

$$\text{where } \lambda_i = \left[\frac{1}{\lambda + c_8 \beta} - \frac{c_9}{\beta^3 + 1} \right]^{-1} \text{ and } \lambda = \frac{R \omega_T}{V_w} = \frac{R a_g \omega_r}{V_w}$$

Here ω_T and ω_r are the angular velocity (rad/s) of the turbine and the generator rotor, respectively. R is the turbine blade length (m) and a_g is the gear ratio. The value of various constants (c_1 – c_9) can be determined from manufacturer data. The above equations are very useful in designing control system of a WT to maximize its efficiency. However, the objective of this paper is to determine the power flow results of a wind integrated power system and the evaluation of control strategy of WT is beyond the scope of the paper.

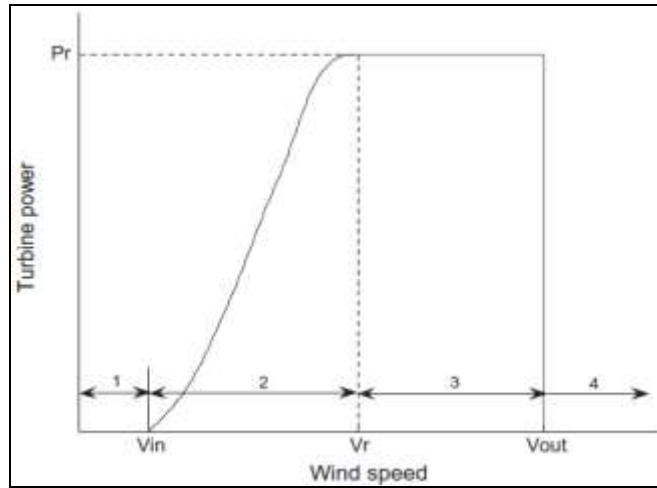


Figure 1: Typical power curve of a wind turbine

A typical variation of turbine power against wind speed is shown in Figure 1 where V_{in} , V_r and V_{out} represent the cut-in wind speed, rated wind speed and cut-out wind speed, respectively, and P_r is the rated power of the turbine. It can be noticed in Figure 1 that the turbine power is variable only in region 2 where the wind speed varies between V_{in} and V_r . In other regions (1, 3 and 4) or wind speeds, the turbine power is either zero or at rated value. Fortunately, most of the WT manufacturers provide the power curve and thus for a given wind speed, the turbine power can immediately be determined from the curve or a lookup table. In simulation studies, it is preferable to have piece-wise mathematical expressions of the power curve. Refs. [20,21] estimated the power in region 2 ($V_{in} \leq V_w \leq V_r$) through a quadratic function using the values of V_{in} , V_r and P_r . In this study, the turbine power P_T in region 2 is expressed by the following polynomial

$$P_T = a_0 + a_1 V_w + a_2 V_w^2 + a_3 V_w^3 \tag{6}$$

The manufacturer data can be used to evaluate the coefficients a_i 's of (6) using any standard curve fitting technique. Figure 2 shows a comparison of estimated power obtained through (6) with the corresponding actual values of Vestas V100-1.8 MW wind turbines supplied by the manufacturer [10]. The coefficients of (6) are obtained through 'polyfit' routine given in MATLAB using the manufacturer data extracted at discrete wind speeds (at an interval of 1 m/s) from cut-in wind speed of 3 m/s to rated wind speed of 12 m/s.

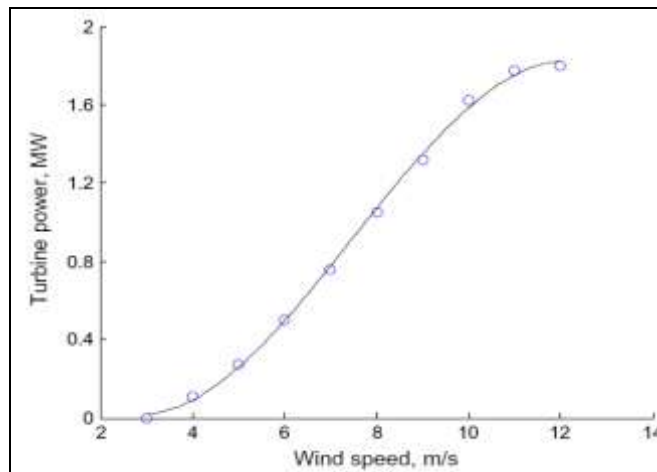


Figure 2: Comparison of estimated and actual turbine power

Thus, mathematically, the turbine power P_T of Figure 1 can be expressed as

$$P_T = \begin{cases} 0; & V_w \leq V_{in} \\ (a_0 + a_1 V_w + a_2 V_w^2 + a_3 V_w^3); & \text{if } V_{in} \leq V_w \leq V_r \\ P_r; & V_r \leq V_w \leq V_{out} \\ 0; & V_w > V_{out} \end{cases} \tag{7}$$

A small fraction of turbine power is lost in the gearbox and the remaining power can be considered as input mechanical power P_m to the generator. Thus,

$$P_m = \eta_g P_T \tag{8}$$

Here η_g is the efficiency of the gear box. The generator converts mechanical power P_m into electrical power and feeds into the grid. The objective of this study is to properly model the WTGS and incorporate the model into a conventional power flow program to evaluate the steady state results of the system.

In the above figure the circles denotes the manufacture given data and the curve denotes the equation 6

4. Model of WTGS and its incorporation into power flow program

We can study the characteristics of the line and power flow in the; ine can be studied by Consider that the SCIG of a fixed speed WTGS is connected to bus k of a general power system through a step-up transformer as shown in Figure 3. An external shunt capacitor is also connected to the generator terminal to supply reactive power. Note that a SCIG always absorbs reactive power and that can be compensated by the external shunt capacitor. Alternatively, a static var compensator (SVC) or a static synchronous compensator (STATCOM) can be used to support reactive power. By selecting appropriate size of shunt capacitors and/or SVC/STATCOM, the terminal voltage of the generator can be regulated.

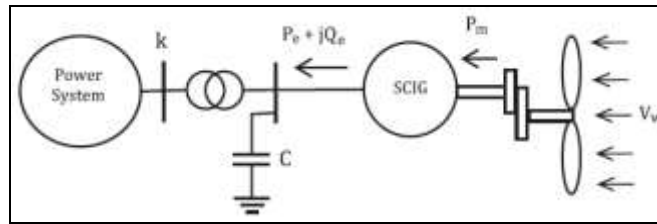


Figure 3. Schematic diagram of a fixed speed WTGS connected to a power system through a transformer

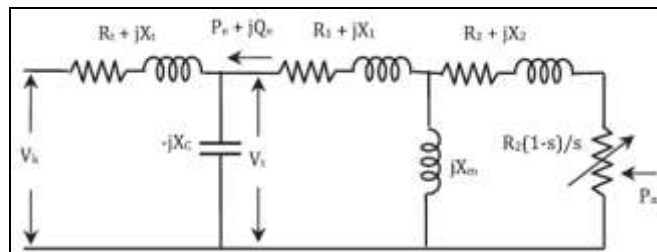


Figure 4. Equivalent circuit of a fixed speed WTGS including the transformer and shunt capacitor

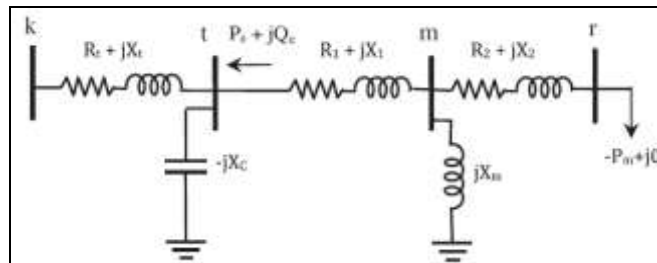


Figure 5. Single-line representation of Figure 4

The equivalent circuit of the SCIG including the transformer and the shunt capacitor is shown in Figure 4 where R_1 , R_2 , X_1 , X_2 and X_m represent the stator resistance, rotor resistance, stator leakage reactance, rotor leakage reactance and magnetizing reactance, respectively, of the generator, and s is the slip. $R_t + jX_t$ and $-jX_c$ represent the impedance of the transformer and the shunt capacitor, respectively. The power of the rightmost resistance $R_2(1-s)/s$ of Figure 4 represents the input mechanical power P_m to the generator and is supplied by the WT. Note that, for generator operation, slip s is negative and thus the power absorbed by the resistance is also negative. By knowing wind speed V_w , P_m can be determined through (7) and (8). The generator converts P_m into electrical power and delivers a complex output power ($P_e + jQ_e$) at its terminal (see Figure 4). The difference between P_m and P_e represents the losses in R_1 and R_2 . Note that the generator draws reactive power from the system and thus Q_e is negative. In fact, $-Q_e$ is the sum of reactive power losses in X_1 , X_m and X_2 . The circuit of Figure 4 is redrawn in Figure 5 by explicitly showing two internal buses (m and r) of the generator in addition to the terminal bus t and the system bus k . Bus m represents the air-gap line, where the magnetizing reactance X_m is connected and bus r represents a fictitious rotor internal bus where the WT supplies mechanical power P_m to the generator. In Figure 5, the power supplied by the WT is represented as negated load of $-P_m + j0$. Most of the previous methods [12–16] considered only the generator terminal bus t and determined the complex power ($P_e + jQ_e$) with some approximations or through significant modifications of computational algorithm of the power flow program

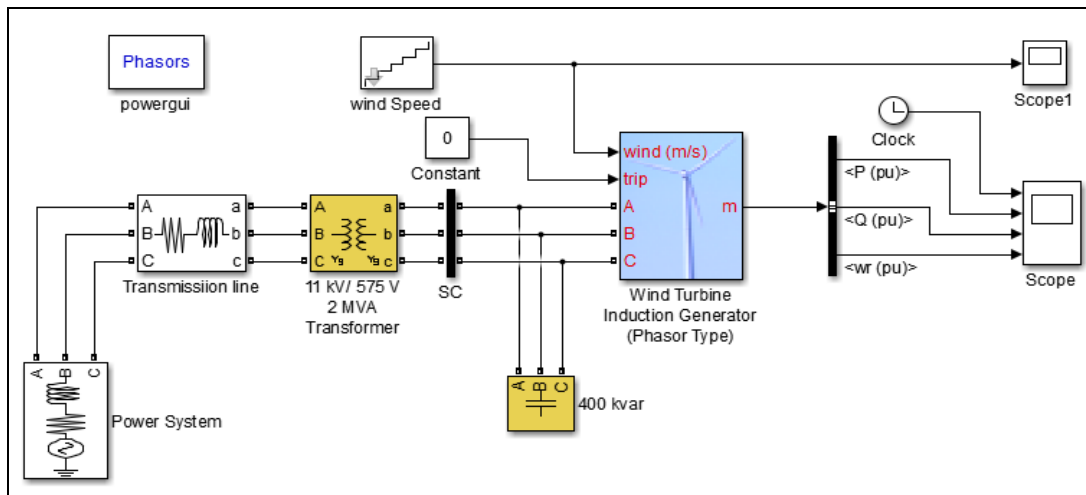


Figure 6: Matlab/Simulink block diagram of the simple system

However, the proposed method extends the generator model beyond the terminal bus to include all parameters of the exact equivalent circuit of the generator. It may be mentioned here that the core loss resistance of the generator can also be included in parallel with jX_m at bus m. By looking into Figure 5, one can easily recognize that it is simply a radial system consisting of four buses (k, t, m and r), three series elements ($R_t + jX_t$, $R_1 + jX_1$ and $R_2 + jX_2$), two shunt elements ($-jX_c$ and jX_m) and a load ($P_m + jQ$) at bus r. The usual values of generator parameters ($R_1 \leq X_1$, $R_2 \leq X_2$, and higher value of X_m) and load at bus r would allow to find the power flow solutions of the system using any standard power flow program by carefully incorporating the parameters of Figure 5 into input data files (bus data and line data) without modifying source codes of the program. Note that a similar model is also used in [22, 23] to represent an induction motor load in determining system loadability through power flow calculations. As mentioned, a power flow program mainly determines the voltage magnitude and phase angle of all buses which are then used to compute power flow of all branches and other quantities. The complex power flow through branch $R_1 + jX_1$ near bus t (as shown in Figure 5) represents the complex power ($P_e + jQ_e$) supplied by the generator at its terminal. The results associated with the internal buses (m and r) of Figure 5 are not important and thus may be ignored or suppressed in the output of the program.

5. Results and discussions

The model of a fixed speed WTGS and its incorporation into a conventional power flow program is vigorously tested on the IEEE 30-bus system. In the IEEE 30-bus system, a number of wind farms (WF) are added throughout the network. It is considered that each wind farm consists of a number of identical Vestas wind turbine (V100-1.8-MW) and SCIG (1.8-MW, 575-V, 0.9-pf) sets. A brief description of wind farms used in this study is given in Table 1. The power curve of the WT is obtained from [10] and it has a cut-in, rated and cut-out wind speed of 3, 12 and 25 m/s, respectively. Even though the curve is for a pitch-controlled variable speed turbine but the same data is used in this study because of the lack of actual data for a large size fixed speed turbine. Ref. [24] demonstrated that the power curve of a pitch-controlled fixed speed WT is not significantly different than that of a variable speed WT.

Wind farm	Number of WT and SCIG sets	Capacity in MW/MVA
A	5	9/10
B	10	18/20
C	15	27/30

Table 1: Summary of various wind farms used in the IEEE 30-bus system

The gear efficiency η_g of the turbine is arbitrarily assumed as 95%. The parameters of the generator are considered as $R_1 = 0.004843$ pu, $X_1 = 0.1248$ pu, $R_2 = 0.004377$ pu, $X_2 = 0.1791$ pu, and $X_m = 6.77$ pu. The leakage reactance of the step-up transformer is assumed as 0.05 pu. The power flow results of the above three systems are obtained by the NR method. The NR power flow program given in PowerToolbox [9] as well as developed in [25] is used for this purpose and both programs provide the same results.

The single line diagram and data of the IEEE 30-bus system are given in [9]. The system is modified by adding three wind farms A, B and C (as described in Table 1) at buses 14, 26 and 30, respectively. The network of the system is then augmented to include the model of the wind farms. In the augmented network, the generator terminal bus (bus t in Figure 5) of wind farms A, B and C is numbered as 31, 34 and 37, respectively. The wind speed of wind farms A, B and C is arbitrarily assumed as 12, 10 and 8 m/s, respectively.

The following are the cases studied in this paper

1. Original system (without wind farms).
2. Modified system without shunt capacitor
3. Modified system with shunt capacitor
4. Modified system at higher wind speeds without shunt capacitor
5. Modified system at higher wind speeds with shunt capacitor

The power flow of the augmented network is then evaluated without and with shunt capacitors. The MVAr rating of shunt capacitors is considered as 25% of respective wind farm capacity in MVA. The power flow of the system is also evaluated at higher wind speeds ($V_r < V_w < V_{out}$) to operate the wind farms at their rated capacity. In all cases, the NR method successfully converged in 4–5 iterations. Table 2 shows a comparison of voltage at system buses 14, 26 and 30 as well as generator terminal buses 31, 34 and 37. The voltage of buses 14, 26 and 30 in the original system (without wind farms) is also shown in the Table for comparison purpose. It can be noticed in Table 2 that the wind farms (without having shunt capacitors) slightly reduce the bus voltage because of drawing reactive power. However, the voltage profile is improved when the shunt capacitors are added. At higher wind speeds (with shunt capacitors), the voltage profile again decreases because of drawing more reactive power.

Bus No	Case 1	Modified System with 3 Wind Farms			
		Case 2	Case 3	Case 4	Case 5
14	1.0429	1.0393	1.0484	1.0385	1.0479
26	1.0025	0.9817	1.0456	0.9726	1.0412
30	0.9953	0.9620	1.0360	0.9566	1.0330
31	-	1.0374	1.0477	1.0366	1.0472
34	-	0.9777	1.0445	0.9677	1.0395
37	-	0.9576	1.0360	0.9522	1.0330
RPL	17.528	14.421	13.487	14.660	13.550

Table 2: Comparison of voltage in per unit at some buses and real power losses (RPL) in MW of the IEEE 30-bus system.

Seller/ Buyer	Case 1	Modified System with 3 Wind Farms			
		Case 2	Case 3	Case 4	Case 5
8/25	21.9	30.7	27.9	32.5	29.6
5/30	14.0	24.8	29.8	23.2	29.8
11/26	11.9	25.8	27.2	20.7	28.7
2/28	13.1	33.8	33.2	34.6	34.1

Table 3: Comparison of ATC in MW of the IEEE 30-bus system

The real power system losses are also shown in the Table 2. It has been observed that the loss reduction is higher when shunt capacitor existing. Table 3 shows the ATC values for the different cases and it has observed the ATC improved in all the cases.

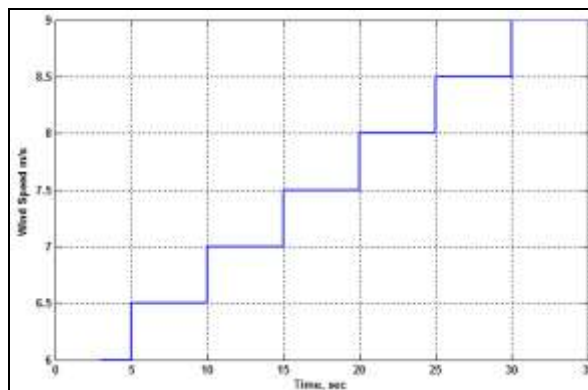


Figure 7: (A) Dynamic responses of the simple system: Wind Speed

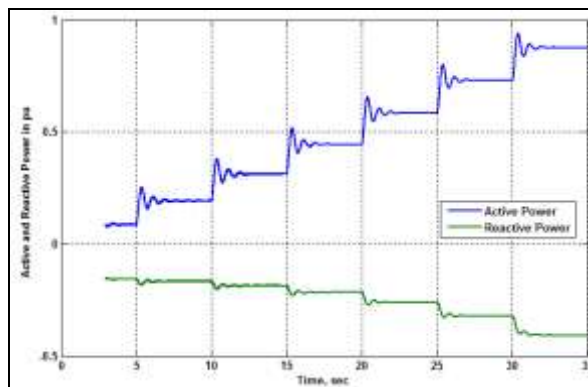


Figure 8: (B) Dynamic responses of the simple system: Active and Reactive Power

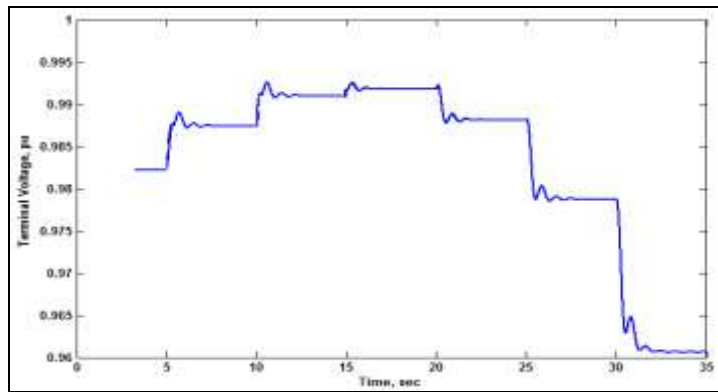


Figure 9: (C) Dynamic responses of the simple system: Terminal Voltage

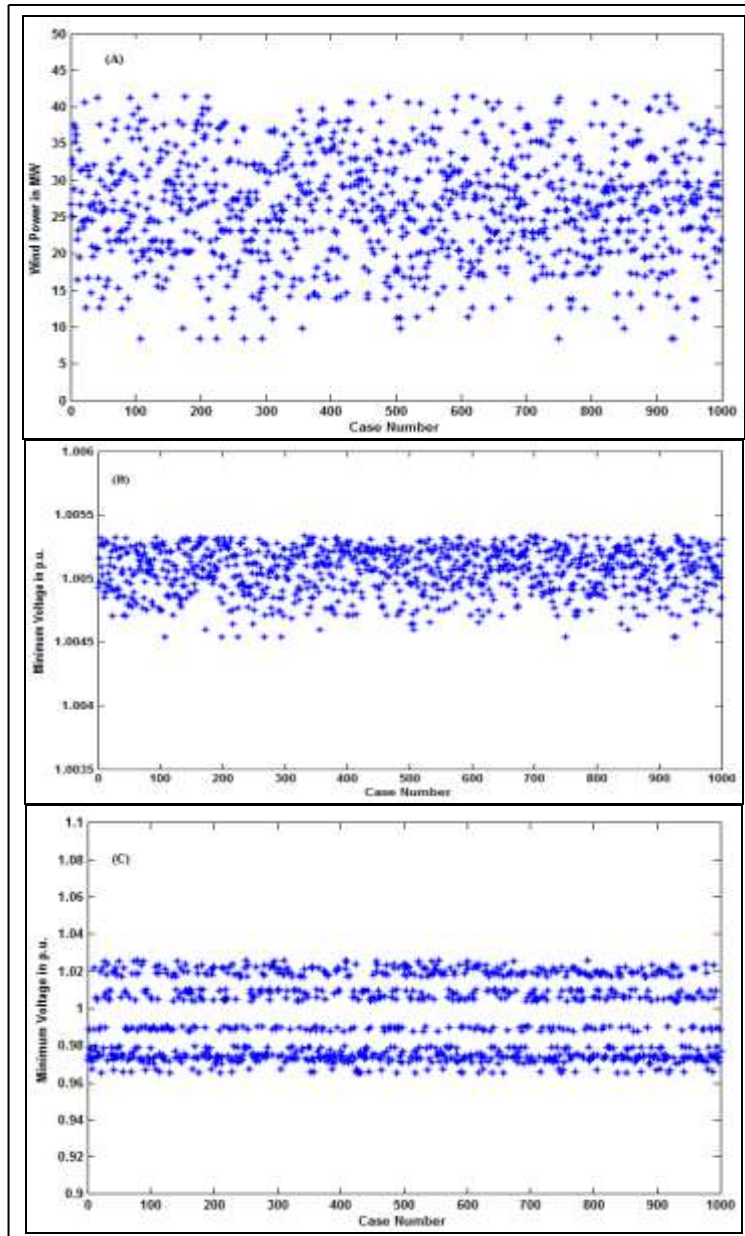


Figure 10: Distribution of results of the 118-bus system for 1000 random cases of wind speeds: (A) wind power, (B) minimum voltage of buses 1–30, (C) minimum voltage in the augmented network.

Finally, the wind speed of all wind farms is randomly selected through Weibull probability density function with a shape parameter of 2 and scale parameter of 9.027 (that corresponds to an average wind speed of 8 m/s [28]) using ‘random’ routine given in Matlab. The power flow problem of the modified network with shunt capacitors is then repeatedly solved for 1000 random cases of wind speeds. In all cases, the NR method successfully converged within 5 iterations. The distribution of total injected wind power (at internal bus r) is shown in Figure 3(A). The minimum and the maximum power for 1000 random cases

are found as 8.52 MW and 41.48 MW, respectively. Note that the total capacity of 3 wind farms is 54 MW. The distribution of minimum bus voltage of the original network (buses 1–30) is shown in Figure 10(B) and it indicates that the minimum voltage varies within a very narrow range (1.0045pu – 1.0053pu) possibly because of low degree of penetration of wind power (<10%). However, the minimum voltage in the augmented network including the generator terminal and internal buses has a wider range (0.9655pu – 1.0258pu) as can be seen in Figure 10(C). In all cases, the lowest voltage occurred at generator internal buses and which is not so important.

6. Conclusions

A simple method of incorporating the exact equivalent circuit of a fixed speed wind generating system into a conventional power flow program has been presented in this paper. The method simply augmented the network by adding two internal buses for each generating system. The new buses have the same property as a P–Q bus and thus can easily be incorporated into any power flow program without modifying the source codes of the program. However, augmentation of input data files of the program is needed to include the model or parameters of the generating system. The effectiveness of the proposed method is well discussed with IEEE 30-bus system. The power flow results of the simple system were also compared with the corresponding steady state values of dynamic responses of the system and are found to be in excellent agreement. It is also found that the incorporation of wind generators does not affect the convergence pattern of the power flow program. ATC also discussed and observed the maximum power flow between the seller and buyer and also variation of the active reactive power and terminal voltages of the system according to the change in wind speed is determined through graphs

7. References

1. Smith JC, Parsons B. Wind integration – much has changed in two years. *IEEE Power Energy Mag* 2011;9(6):18–25.
2. <<http://www.thewindpower.net/index.php>>.
3. Li H, Chen Z. Overview of different wind generator systems and their comparisons. *IET Renew Power Gener* 2008;2(2):123–38.
4. IEEE PES Wind Plant Collector System Design Working Group. Characteristics of wind turbine generators for wind power plants. In: Proc. 2009 IEEE power and energy society general meeting, Calgary, Canada, July 2009.
5. Muljadi E, Butterfield CP. Pitch-controlled variable-speed wind turbine generation. NREL, Report No. NREL/CP-500-27143, 2000.
6. Slootweg JG, Polinder H, Kling WL. Representing wind turbine electrical generating systems in fundamental frequency simulations. *IEEE Trans Energy Conversion* 2003;18(4):516–24.
7. Hansen AD, Hansen LH. Wind turbine concept market penetration over 10 years (1995–2005). *Wind Energy* 2007;10:81–97.
8. Kundur P. Power system stability and control. McGraw-Hill; 1993.
9. Sادات H. Power system analysis. McGraw-Hill; 1999.
10. <<http://www.vestas.com/en/media/brochures.aspx>>.
11. <<http://www.energy.siemens.com/mx/en/power-generation/renewables/wind-power/wind-turbines/>>.
12. Feijoo AE, Cidras J. Modeling of wind farms in the load flow analysis. *IEEE Trans Power Syst* 2000;15(1):110–5.
13. Eminoglu U. Modelling and application of wind turbine generating systems (WTGS) to distribution systems. *Renew Energy* 2009;34:2474–83.
14. Divya KC, Rao PSN. Models for wind turbine generating systems and their application in load flow studies. *Electric Power Syst Res* 2006;76: 844–56.
15. Liu Y, Wang W, Xu L, Ni P, Wang L. Research on power flow algorithm for power system including wind farm. *ProcIntConf Electric Mach Syst* 2008:2551–5.
16. Feijoo A. On PQ models for asynchronous wind turbines. *IEEE Trans Power Syst* 2009;24(4):1890–1.
17. Esquivel CRF, Hernandez JHT, Alcaraz GG, Torres FC. Discussion of modelling of wind farms in the load flow analysis. *IEEE Trans Power Syst* 2001;16(4):951.
18. Heier S. Grid integration of wind energy conversion systems. 2nd ed. John Wiley; 2006.
19. Ackermann T. Wind power in power systems. John Wiley; 2006.
20. Pallabazzer R. Evaluation of wind-generator potentiality. *Sol Energy* 1995;55(1):49–59.
21. Villanueva D, Pazos JL, Feijoo A. Probabilistic load flow including wind power generation. *IEEE Trans Power Syst* 2011;26(3):1659–67.
22. Martins N, Henriques RM, Barbosa AA, Gomes S, Jr, Gomes CB, Martins ACB. Impact of induction motor loads in system loadability margins and damping of inter-area modes. In: Proc. of the IEEE PES General Meeting, vol. 2, 2003. p. 1379–84.
23. Henriques R, Martins N, Ferraz JCR, Martins ACB, Pinto HJPC, Carneiro S, Jr. Impact of induction motor loads into voltage stability margins of large systems. In: Proc. of power systems computations conference, Seville, Spain, 2002.
24. Burton T, Jenkins N, Sharpe D, Bossanyi E. Wind energy handbook. 2nd ed. John Wiley; 2011.
25. Haque MH. Novel decoupled load flow method. *IEE Proc C* 1993;140(3):199–205.
26. SimPowerSystems User's Guide, MathWorks, 2012.
27. Haque MH, Rahim AHMA. Determination of first swing stability limit of a multimachine power systems. *IEE Proc C* 1989;136(6):373–9.
28. Masters GM. Renewable and efficient electric power systems. Wiley Interscience; 2004
29. Nireekshana T, KesavaRao G, Sivanagaraju S. Enhancement of ATC with FACTS devices using Real coded genetic algorithm. *International Journal of Electrical Power and Energy Systems* 2012;43:1276-1284